Supplemental Information

Understanding Membrane-active Antimicrobial Peptides

Huey W. Huang and Nicholas E. Charron
Department of Physics and Astronomy, Rice University, Houston, Texas 77005

This supplemental information provides comments on sample preparation and experimental procedures for the studies that have been done in support of this review. We feel that it is important to reiterate and demonstrate the importance of sample preparation and quality, as well as some not commonly discussed aspects of the associated methods. We focus primarily on the techniques related to multilayer samples, as structure/state determination of a soft matter peptide-membrane system is susceptible to several subtle but important pitfalls.

S1. Comments on sample preparation

Good sample quality is crucial for the success of experiments that investigate membrane active agents. This is in part due to the inherent difficulty of studying single membranes with traditional physical techniques. In particular, a single bilayer supported on a solid substrate is known to have its properties altered from that of a free bilayer in solution (Hemmerle et al., 2012). An ideal alternative is a stack of parallel bilayers of lipid-peptide mixtures separated by water layers, equivalent to a smectic liquid crystal. However, lipids have a molecular basis for a very rich lyotropic liquid crystal phase diagram that depends heavily on both temperature and hydration. There are many types of defects that can span over a variety of length scales. Due to the birefringence of optical artifacts, polarizing microscopy can be used to qualitatively identify and characterize defects in multilayer samples (Powers & Pershan, 1977). X-ray can also be used to measure sample alignment and homogeneity, as well as detecting the formation of phase domains. Thus rejection of poor samples should be a routine and well-defined process in X-ray, neutron, and OCD experiments.

The quality of GUVs is a little less straightforward to ascertain. GUVs seem to be considerably more fragile than biological membranes (the reason for which is still not entirely certain) (Faust et al., 2017). GUVs with diameters on the order of one to tens of microns should be able to withstand reversible membrane tensions on the order of mN/m (Lee et al, 2013). GUVs are typically produced in ~ 200 mM sucrose (or glucose) and immersed in ~200 mM glucose (or sucrose) solution. The high concentrations of sugar control the osmolalities so as to withstand modest osmotic downshifts and upshifts. The choice of sucrose and glucose provides phase contrast for microscopic observation and also provide a density differential to control the vertical position of GUVs in the observation chamber.

Multilayer Sample Preparation

As stated earlier, well defined sample preparation is key to studying AMPs with precision. Methods such as X-ray diffraction and OCD require uniform and well-aligned samples to provide good signal to noise ratios, and the accurate extraction of peptide behaviors from these techniques

require good sample alignment. X-ray diffraction is especially sensitive to sample quality, and direct measurements can unambiguously detect samples with poor alignment, non-uniformity or phase separations.

Generally, there are two methods for diffraction/OCD multilayer sample preparation. The first involves the use of organic solvents to mix and spread compounds on substrates (silicon wafer, glass, or quartz). Lipids and additional components are first co-dissolved in a mixture of organic solvents and pipetted onto cleaned substrate. Either by hand or by some form of auto-nutation/rotation, the substrates carrying the deposited solution can be gently rocked or gyrated to spread the sample evenly while the solvents evaporate. Liquid surface tension and contact angle play a critical role in this process; the ideal solution is tensionless to allow for natural spreading across the substrate, so solvents may be chosen at ratios that produce this characteristic behavior (Ludtke et al., 1995). Generally, a hydrophobic solvent can be used to dissolve the lipid-peptide mixture, while an amphipathic solvent promotes sufficient spreading over the substrate surface. Common solvent choices are chloroform, trifluoroethanol, and/or methanol.

After most of the solvent has evaporated and the sample is uniformly distributed on the substrate, the substrate may be set aside to allow the remainder of the solvent to evaporate. It is usually necessary to remove all traces of the solvent after spreading, so samples are placed under vacuum for at least an hour after the mixing. Once all of the solvent has been removed, the substrates with dried sample are incubated and slowly rehydrated in the presence of purified water vapor (preferably over night), after which they may be mounted for diffraction or OCD experiments.

A major caveat for preparing multilayer samples with organic solvents is solubility. In order to produce well-mixed samples, all components must be soluble in the final solvent mixture. For simple mixtures and samples of pure lipid this is hardly an issue. However, more complicated lipid-peptide-sterol systems can often present the experimenter with a difficult problem in miscibility. Just as well, additional components, such as ions, may not be well incorporated using organic solvent methods and the uniformity of their distributions throughout the sample is not guaranteed. Additionally, mixed solvents with different evaporation rates may leave an experimenter with an initially well mixed sample that evolves to a poorly mixed one. Often the solution to this problem involves substantial trial and error concerning solvent types and mixing ratios.

The second method of multilayer preparation addresses some of these issues. This method involves the lyophilization of the sample into a powder form that may subsequently be rehydrated (Huang & Olah, 1987; Olah et al., 1991). First, dissolved lipids are dried down to a film and placed under vacuum. Next, the lipid film is mixed with some volume of pure water and is vortexed and sonicated to produce vesicles. Additional components, such as peptides, ions, or sterols, may be spiked in the resulting solution. This solution is vortexed and sonicated yet again to produce a uniform distribution. The solution is then frozen in preparation for lyophilization. Once frozen, the solution is placed under a cold vacuum until all water content is removed via sublimation and an anhydrous powder is produced. Typically, this process may be done

overnight. The resulting dried samples may be incubated and rehydrated with pure water to form a translucent gel-like substance. It is important to note that this hydration must be sufficiently quasi-static; if the hydration is too sudden (as a result from, for example, water droplets landing directly on the anhydrous powder), then a colloidal suspension of vesicles will be produced, instead of a well-aligned sample. This is often evidenced by a sticky and viscous solution that is opaque, off-white in color, rather than a translucent and easily partitionable gel.

The rehydrated lyophilized samples may be spread onto substrate using a small spatula. Gentle spreading will result in a visibly uniform conic-fan texture that is characteristic of the lipids' smectic liquid crystalline behavior (Kumar, 2001). Depending on the lipid mixture, the spreading process may be augmented by use of a glovebox with ambient humidity control and a controllable heater that makes thermal contact with the substrate. Alternatively, rehydrated samples may be sandwiched between two clear substrates (for OCD or neutron) or polished beryllium plates (X-ray) that are gently rubbed together with slight compression. This gentle pressure and rubbing can be used to localize multilayer defects to the edges of the substrate, and the presence of two bounding surfaces promotes the propagation of uniform lamellar order across the sample (Powers & Pershan, 1977). Samples that have been spread may be stored in incubation and further hydrated using pure water vapor in the same fashion as the samples prepared via organic solvents.

If the samples are prepared on glass, the alignment and domain quality may be investigated with the use of a polarizing microscope (Huang & Olah, 1987; Powers & Pershan, 1977). Lamellar lyotropics show clear birefringence associated with axes parallel and perpendicular to the layer normal. Lamellar X-ray diffraction can also measure sample quality, as a well-aligned sample will have a good signal to noise ratio, and, at less than full hydration, typically more than four Bragg orders with sharp diffraction peaks. A θ–2θ scan can reveal any phase separation--a phenomenon marked by the appearance of more than one series of peaks with different repeat distances. The mosaic quality may be more carefully inspected with a two-dimensional rocking (ω, θ) scan centered about a chosen Bragg peak. A sample that has poor layer alignment shows no omega dependence in the intensity of the scan, a feature characteristic of powder samples, and is marked by the appearance of an extremely wide Gaussian peak along the omega axis. By contrast, a well aligned sample has a sharp omega dependence in the intensity that is focused in a narrow Gaussian peak about the center of the Bragg peak under inspection (Weiss et al., 2003).

S2. Comments on methods

S2.1 GUV in peptide solution—aspiration method

The aspiration method (Kwok & Evans, 1981) measures the membrane area change by peptide binding, from which one can find, by its correlation with the membrane thinning effect measured with X-ray diffraction, the number of peptides bound to the GUV membrane (the bound peptide to lipid ratio) during the experiment (Sun et al., 2009)).

When a GUV is exposed to pore-forming peptides, the initial binding of peptides always expands the membrane area of the GUV, resulting in an increased protrusion length in the

aspiration micropipette (Lee et al., 2008; Longo et al., 1998; Longo et al., 1997; Sun et al., 2009). The simplest explanation for this is that additional molecules have been incorporated into the lipid bilayer. The subsequent pore formation causes a net water influx if, for example, sucrose and glucose are used as the solutes inside and outside the GUV, respectively. This would cause a decreased protrusion length (Lee et al., 2011; Lee et al., 2013; Longo et al., 1998; Longo et al., 1997; Sun et al., 2009), because glucose is smaller than sucrose, leading to a slightly larger glucose influx than a sucrose eflux which in turn produces a net water influx due to osmolality imbalance (Longo et al., 1998). If the sucrose and glucose were exchanged, the pore formation would cause a net water efflux, resulting in an increased protrusion length (Sun et al., 2009).

S2.2 Measurement of instantaneous membrane permeability

Membrane permeability induced by AMPs is most commonly measured by molecular leak-in or leak-out methods (Fuertes et al., 2010; Tamba et al., 2010; Tamba & Yamazaki, 2005). For instance, the time curve for the dye release can be measured from a GUV or from a population of small vesicles. However, the membrane permeability induced by AMPs in solution changes with time, as the peptides gradually bind to the membrane. A single time curve of efflux or influx does not reveal such time dependent changes. If it is the collective efflux from a population of small vesicles, the kinetics can be complicated by the ensemble average and by the molecular exchange between vesicles by collision (Martin & Pagano, 1987; Rodriguez et al., 2005; Seigneuret & Devaux, 1984). In (Faust et al., 2017; Sun et al., 2016), we have shown that, by photobleaching and fluorescence recovery in a leak-in experiment, we can measure the instantaneous permeability in a bacterial membrane by using spheroplasts or in a lipid bilayer by using GUVs.

S2.3 Oriented circular dischroism (OCD)

The method of OCD is perhaps the simplest way of measuring the configuration and orientation of peptides in membranes (Wu et al., 1990). Other methods that have been used for the same purpose include solid-state NMR (Bechinger et al., 1991; Glaser et al., 2004) and polarized infrared spectroscopy (Rothschild et al., 1980; Tamm & Tatulian, 1997). For the comparison of the uses of OCD and ssNMR, see (Burck et al., 2008).

The UV CD spectra of polypeptides and proteins are dominated by the electronic transitions in the peptide backbone and are relatively independent of the side chains. The asymmetric and periodic arrangements of peptide units in secondary structures give rise to characteristic CD spectra. In particular, the α-helix conformation has a highly distinctive spectrum. Within the UV range of commercial CD spectrometers ($\sim 185 - 240\ nm$), the helical spectrum is dominated by the π-π^* and n- π^* transitions (Woody, 1985). According to the exciton theory of Moffitt (Moffitt, 1956), the π-π^* transition in an α-helix is split into components with polarization either perpendicular or parallel to the helical axis. This theory was difficult to prove experimentally due to the difficulty of aligning a sample of α-helices. The use of long polypeptides in an electric field led to conflicting results (Yamaoka et al., 1986), because the

bending of long polypeptides was not taken into account (Olah & Huang, 1988a). Moffitt's prediction on polarization was finally demonstrated experimentally by using membrane-spanning α-helices aligned in lipid multilayers (Olah & Huang, 1988a; Olah & Huang, 1988b). Indeed, stacked lipid bilayers provides an ideal scaffolding for aligning short peptides and membrane-spanning proteins. Clearly the method used to prove the Moffitt theory can be utilized to measure the orientation of the helical sections of membrane proteins. The theoretical basis for the OCD method is given in Wu et al. (Wu et al., 1990). Here we provide some practical information for the use of OCD.

OCD of α-helices

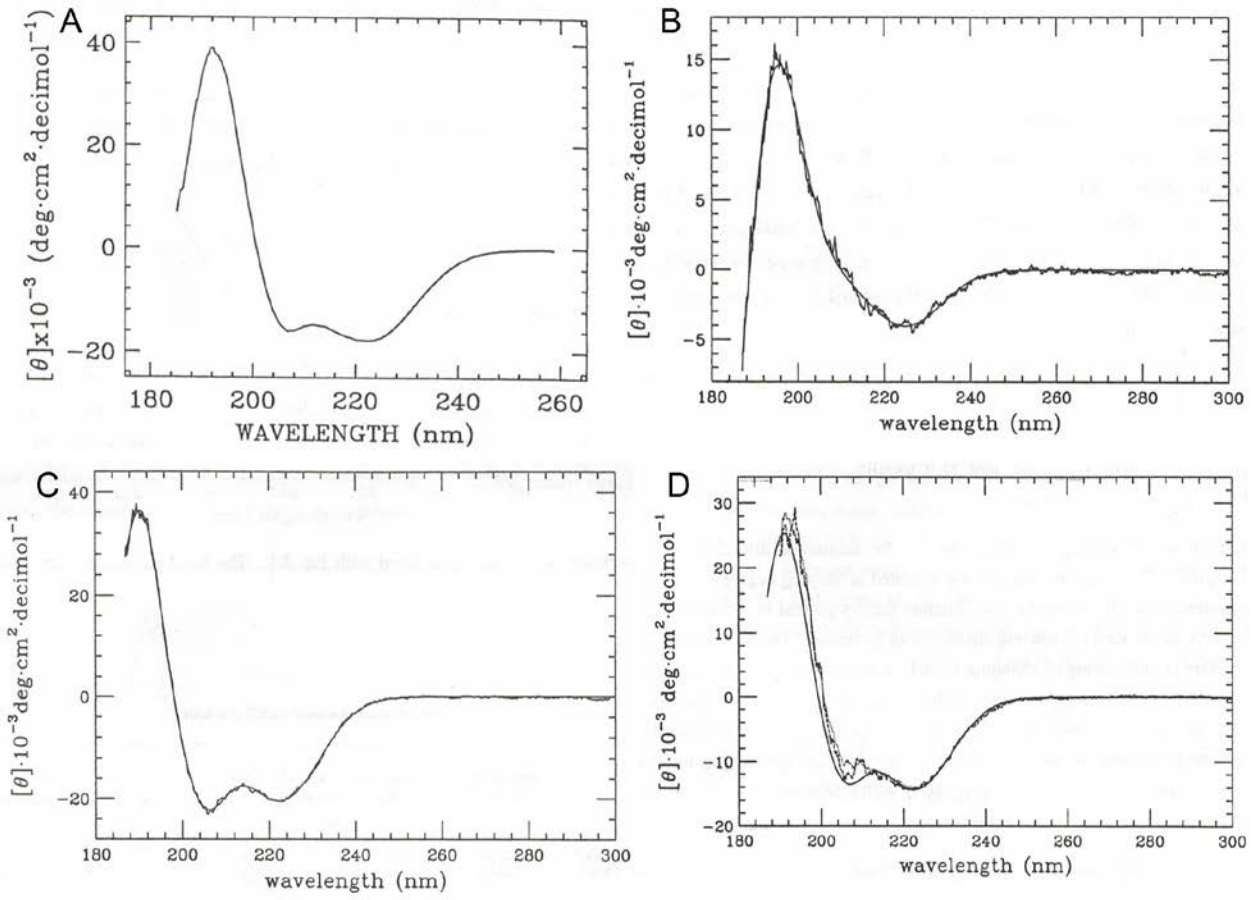

Figure S1 Solution CD and OCD of alamethicin. (A) The solution CD of alamethicin embedded in DPhPC vesicles. (B) OCD of alamethicin in DPhPC multilayers in full hydration. Alamethicin helix is oriented perpendicular to the plane of bilayers—this is called the I state. (C) OCD of alamethicin in DPhPC multilayers in low hydration (~ 50% RH). Alamethicin helix is oriented parallel to the plane of membrane—this is called the S state. (D) The solution CD is the rotational average of the S and I state: $(\frac{1}{3}I + \frac{2}{3}S)$ constructed from (B) and (C) shown in dotted line, compared with the directly measured solution CD in solid line (same as A).

Fig. S1 (Wu et al., 1990) shows the solution CD of alamethicin embedded in lipid vesicles. The negative CD band near 224 nm is due to the n-π^* transition of a magnetic dipole transition moment directed along the carbonyl bond in the helix; the band is approximately a Gaussian. The π-π^* transition in a helix, however, splits into three: one has its electric transition dipole polarized parallel to the helical axis and gives rise to the negative Gaussian band near 205 nm; the other two have their electric transition dipoles polarized perpendicular to the helical axis, giving rise to a positive Gaussian band near 190 nm when the incident light is perpendicular to the helical axis, but, when the incident light is parallel to the helical axis, the two transitions combine to produce the shape of the derivative of a Gaussian centered near 190 nm with the positive amplitude on the long wavelength side called the helical band (Tinoco, 1964). (Note that the CD spectra of short helical peptides are similar but vary somewhat in the relative amplitudes of different bands—this variation does not affect the determination of orientation.)

In contrast to solution CD, OCD is measured with the incident light perpendicular to the oriented multilayers. An example of alamethicin in DPhPC is shown in Fig 9B and 9C (Wu et al., 1990). Alamethicin changes its orientation when the sample's hydration condition changes. At full hydration, the alamethicin helix is oriented perpendicular to the plane of bilayer; the incident light is parallel to the helical axis, the positive band near 190 nm is red shifted (the helical band has a negative band blue shifted to below 190 nm which is difficult to detect by commercial CD spectrometers), the 205 nm band diminishes and the 224 nm band becomes smaller compared with the solution CD—this is called the I state (Fig. 9B). At low hydration (~50% RH), alamethicin helix is oriented parallel to the plane of membrane, i.e., the incident light is perpendicular to the helical axis, there are one positive band at 190 nm, a negative band at 205 nm and a negative band at 224 nm (Fig. 9C). This is called the S state. In solution CD, the observed signal is the rotational average of the S and I state ($\frac{1}{3}I + \frac{2}{3}S$), which agrees with the directly measured solution CD (Fig. 9D). Because the amplitudes associated with S are larger than that of I, the S state is similar to the solution CD (the distinction is the more negative amplitude at 205 nm). If a peptide has only two stable orientations, then the OCD of any mixed state exists as a linear combination of the I and S states. (A mixed state can also be interpreted as a helix at a tilted angle (Wu et al., 1990), but we believe that a peptide having multiple stable tilt-angle states is unlikely.)

OCD of β-sheets.

The OCD theory for β-sheets is less well developed (Bazzi & Woody, 1987; Woody, 1993) compared with α-helices. Nevertheless OCD has been used to establish two distinct states of protegrin (Ding et al., 2003; Heller et al., 1998) and θ-defensins (Weiss et al., 2002) in membranes.

Practical OCD analysis.

Ideally one would like to obtain both the S and I spectra from one single sample, so that they are normalized relative to each other. In this case, the OCD of the peptide in any condition

can be decomposed into a linear combination of S and I states, from which the percent of the peptide in each orientation is determined. This is done by searching two extreme spectra in the sense that all other spectra fall in between and can be expressed as a linear combination of the two. The extreme spectra have been found by measuring the OCD of a peptide in different lipid bilayers, P/L ratios, degrees of hydration and temperatures (Heller et al., 1998; Huang & Wu, 1991; Ludtke et al., 1994; Weiss et al., 2002; Yang et al., 2001). One learns a great deal about the peptide of interest by these relatively simple measurements.

Even if one fails to obtain both S and I in one single sample, it is still possible to normalize S and I obtained from two different samples in different conditions by an isodichroic point. Suppose that there is a cross point between the mutually normalized S and I spectra, then this isodichroic point must be common to all spectra provided they are all normalized correctly. One can usually find such a point by varying the hydration or temperature of one sample. The relative normalization between different samples is then achieved by adjusting the ampltidues of all other spectra to cross this isodichroic point.

OCD distortion

The original paper on OCD discussed the possible artifacts of OCD measurement and the techniques for correction (Wu et al., 1990). In practice, the most common distortion of OCD spectra is due to sample defects. If the multiple bilayers in the sample are not well aligned (as determined by X-ray, for example), the OCD spectrum would appears normal, but the deduced peptide orientation would be erroneous. This is generally true for any method of peptide orientation measurement. Another commonly seen OCD distortion comes from a sample not spread uniformly over the substrate resulting in non-uniform thickness. In a severe case the amplitude would taper to zero as wavelength decreases. The following explanation makes this clear.

Modern CD spectroscopy is based on a polarization-modulation technique (Velluz et al., 1965). A linearly polarized light is modulated alternatively into the right and left circularly polarized light before passing through the sample. Thus the readout, i.e., the voltage output, consists of an AC component proportional to the AC component of the transmitted light I_{ac} and a DC component proportional to the average transmitted light I_{dc} ($I_{dc} >> I_{ac}$). The ellipticity is measured by the ratio of the AC component over the DC component I_{ac}/ I_{dc} (Velluz et al., 1965). This ingenious design makes the measured ellipticity (or CD) independent of the sample's optical absorption which increases drastically as the wavelength decreases below ~200 nm. Now, to illustrate the CD distortion by a non-uniform sample, imagine a sample does not cover the entire substrate, so the transmitted light consists of two parts, $(I_{ac} + I_{dc})_A$ and $(I_{dc})_B$; the B part has no AC component because it has no sample. The output of the CD measurement would then be $(I_{ac})_A/[(I_{dc})_A + (I_{dc})_B]$. As long as the sample absorption is relatively independent of wavelength this output would still produce a correct unnormalized CD spectrum (for example in the wavelength region above ~200 nm). However, below 200 nm the components $(I_{ac})_A$ and $(I_{dc})_A$ would exponentially decrease with the wavelength due to UV absorption by the sample, while the

component $(I_{dc})_B$ would remain as large as above 200 nm because there is no sample absorption. Thus, such a spectrum would be distorted.

S2.4 X-ray lamellar diffraction

There are two standard types of diffraction samples (Warren, 1990). One type is powder and another is crystalline. For lipid bilayers, a powder sample corresponds to collection of small multilayered vesicles. Diffraction peaks from such samples rarely show the full circles of diffraction patterns (as a perfect powder would), indicating a lack of isotropy, and are typically limited to 4 orders of Bragg peaks, which is insufficient for precise measurements. On the other hand, it is relatively easy to prepare the so-called "ideally imperfect" (Warren, 1990) smectic liquid crystalline samples as described in Section S1.

As mentioned previously, lamellar diffraction can be used to measure a peptide's effect on the thickness of the bilayer, its dependence on P/L, and the value of P/L*. Levine and Wilkins (Levine & Wilkins, 1971) carried out the first structural x-ray diffraction experiments on lipid bilayers, identifying distinct hydrocarbon chain and phosphate head group regions. The basic method exploits the one-dimensional periodicity of the multilamellar phase. In this liquid crystalline form, the unit cell is taken to be a bilayer and half of both sides of the surrounding water layers. These multilayer samples may be probed with simple θ–2θ scans.

The observed diffraction peaks must be adjusted with several physical and geometrical corrections. This first of these involves the removal of the background signal. The next correction applies to the absorption of the sample. This is perhaps one of the more difficult corrections to compute, as determining the exact number of parallel bilayers are present in the sample is nontrivial. However, if the thickness of the sample d is known, the absorption correction is simple (Warren, 1990): $C_{abs} = \left(\frac{sin\theta}{2\mu d}\left[1 - \exp\left(-\frac{2\mu d}{sin\theta}\right)\right]\right)$,

where μ, the sample absorption coefficient is simply the mass weighted sum of atomic coefficients based on the chemical formulas of the compounds that comprise the sample.

Next, a polarization correction must be made as well. Commercial x-ray tubes produce completely unpolarized radiation, which in the geometry of a θ–2θ scan results in a polarization factor of (Warren, 1990) $C_p = (1 + cos^2 2\theta)/2$. However, if a monochromator used in front of the detector, the polarization factor is $C_p = (1 + cos^2 2\theta cos^2 2\theta_{mono})/2$.

Lastly there is the Lorentz factor. This factor comes about because the theoretical diffraction peak amplitude is integrated over the q space, where as the measurement is integrated by the detector surface as well as the ω rotation during the θ–2θ scan (Warren, 1990). As a result the measured diffraction intensity is the theoretical intensity multiplied by the Lorentz factor $C_L = 1/sin2\theta$ (for the lamellar diffraction). All together the measured intensity is proportional to $|F|^2 \cdot C_{abs} \cdot C_p \cdot C_L$ where F is the diffraction amplitude.

The electronic density of the unit cell can be constructed once the amplitudes of each Bragg peak have been corrected. As with all x-ray structure determinations however, the true challenge lies in the determination of phases for each Bragg peak amplitude. The centro-

symmetry of the unit cell guarantees that phases will be either $+1$ or -1. Blaurock introduced a straightforward method for phase determination of multilamellar samples based of unit cell modulation (Blaurock, 1971). In this method, the thickness of the water layer (and hence the unit cell D-spacing) is changed via humidity control of the sample in the lamellar phase. Data taken from multiple samples or humidities may be normalized using yet another method introduce by Blaurock (Blaurock, 1971). One can then overlay experimentally obtained rescaled structure factors from different humidities, and the phases may be determined accordingly from the set that most accurately traces out the structure factor curve.

This method assumes that the overall structure of the unit cell (particularly the bilayer) remains unchanged aside from thickening/thinning the water layers at different relative humidities (Torbet & Wilkins, 1976). Discrete Fourier inversion, with the proper choice of phases, can produce electron density profiles of the unit cell. The extrapolated the bilayer thickness at full hydration is measured as the distance between the two reconstructed phosphate peaks, or the PtP distance. The observed dependence of the PtP distance on D-spacing (and hence humidity) is non-linear monotonic decreasing and approaches an asymptotic value as the D-spacing increases. This asymptotic value is taken as the bilayer thickness at full hydration.

The one-dimensional electron density profiles of the lamellar phase recovered from diffraction experiments have a characteristic shape and carry useful qualitative information beyond the numerical measurement of the PtP distance. In particular, the acyl chain region of the bilayer undergoes disorder changes as relative humidity changes. At lower relative humidities, finer features can be seen in the acyl chain region as the chains have greater correlated order in packing and tilt angles. By contrast, the acyl chain regions at higher relative humidities are much smoother, indicating more disorder in packing and tilt angles. Qualitatively, these changes may be taken as evidence that the multilayer is swelling properly with hydration, though some agents, such as cholesterol or ergosterol, can modify this general behavior when incorporated into the samples (Hung et al., 2007; Hung et al., 2016).

S2.5 Neutron in-plane scattering: detecting and sizing transmembrane pores, see (Ding et al., 2004; He et al., 1996; Huang & Yang, 2009; Yang et al., 1998).

S2.6 Multiwavelength anomalous diffraction: lipidic structure of the pores, see (Huang, 2012; Qian et al., 2008; Wang et al., 2006; Yang & Huang, 2003).

Movie S1

The movie of Figure 2. (The red line on the micropipette is an optical artifact.) At the beginning, the GUV of DOPC/DOPG 7:3 is seen by the red color of the soluble dye TRsc (MW 625, 10 μM) inside the GUV. The appearance of green on the surface of GUV indicates the binding of FITC-melittin (2 μM) outside the GUV. The binding causes the area expansion hence the protrusion in the micropipette increases. Then the intensity of red color suddenly begins to decrease and diminish, indicating the formation of stable pores in the membrane. For a while the protrusion length continued to increase due to further binding of melittin. As explained in the

section **S2.1,** the formation of stable pores causes the GUV to swell, because of our initial preparation with sucrose inside versus glucose outside the GUV. After the melittin binding reaches equilibrium the protrusion length eventually decreases due to the GUV volume increase. The real time of the movie is 400s total. Photobleaching was negligible. (Lee et al., 2013)

References

BAZZI, M. D. & WOODY, R. W. (1987). Interaction of Amphipathic Polypeptides with Phospholipids - Characterization of Conformations and the Cd of Oriented Beta-Sheets. Biopolymers, 26(7), 1115-1124.

BECHINGER, B., KIM, Y., CHIRLIAN, L. E., GESELL, J., NEUMANN, J. M., MONTAL, M., TOMICH, J., ZASLOFF, M. & OPELLA, S. J. (1991). Orientations of amphipathic helical peptides in membrane bilayers determined by solid-state NMR spectroscopy. J Biomol NMR, 1(2), 167-173.

BLAUROCK, A. E. (1971). Structure of the nerve myelin membrane: proof of the low-resolution profile. J Mol Biol, 56(1), 35-52.

BURCK, J., ROTH, S., WADHWANI, P., AFONIN, S., KANITHASEN, N., STRANDBERG, E. & ULRICH, A. S. (2008). Conformation and membrane orientation of amphiphilic helical peptides by OCD. Biophys J, 95, 3872-3881.

DING, L., LIU, W., WANG, W., GLINKA, C. J., WORCESTER, D. L., YANG, L. & HUANG, H. W. (2004). Diffraction techniques for nonlamellar phases of phospholipids. Langmuir, 20(21), 9262-9269.

DING, L., YANG, L., WEISS, T. M., WARING, A. J., LEHRER, R. I. & HUANG, H. W. (2003). Interaction of antimicrobial peptides with lipopolysaccharides. Biochemistry, 42(42), 12251-12259.

FAUST, J. E., YANG, P. Y. & HUANG, H. W. (2017). Action of antimicrobial peptides on bacterial and lipid membranes: a direct comparison. Biophys J, 112, 1-10.

FUERTES, G., GARCIA-SAEZ, A. J., ESTEBAN-MARTIN, S., GIMENEZ, D., SANCHEZ-MUNOZ, O. L., SCHWILLE, P. & SALGADO, J. (2010). Pores formed by baxalpha5 relax to a smaller size and keep at equilibrium. Biophys J, 99(9), 2917-2925.

GLASER, R. W., SACHSE, C., DURR, U. H., WADHWANI, P. & ULRICH, A. S. (2004). Orientation of the antimicrobial peptide PGLa in lipid membranes determined from 19F-NMR dipolar couplings of 4-CF3-phenylglycine labels. J Magn Reson, 168(1), 153-163.

HE, K., LUDTKE, S. J., WORCESTER, D. L. & HUANG, H. W. (1996). Neutron scattering in the plane of membranes: structure of alamethicin pores. Biophys J, 70(6), 2659-2666.

HELLER, W. T., WARING, A. J., LEHRER, R. I. & HUANG, H. W. (1998). Multiple states of beta-sheet peptide protegrin in lipid bilayers. Biochemistry, 37(49), 17331-17338.

HEMMERLE, A., MALAQUIN, L., CHARITAT, T., LECUYER, S., FRAGNETO, G. & DAILLANT, J. (2012). Controlling interactions in supported bilayers from weak electrostatic repulsion to high osmotic pressure. Proc Natl Acad Sci U S A, 109(49), 19938-19942.

HUANG, H. W. (2012). Diffraction Methods for Studying Transmembrane Pore Formation and Membrane Fusion. In Encyclopedia of Biophysics (ed. G. Roberts), pp. 460- 472 Berlin Heidelberg: Springer-Verlag

HUANG, H. W. & OLAH, G. A. (1987). Uniformly oriented gramicidin channels embedded in thick monodomain lecithin multilayers. Biophys J, 51(6), 989-992.

HUANG, H. W. & WU, Y. (1991). Lipid-alamethicin interactions influence alamethicin orientation. Biophys J, 60, 1079-1087.

HUANG, H. W. & YANG, L. (2009). X-ray methods for investigation of structures of lipid assemblies. In Handbook of Molecular Biophysics (ed. H. G. Bohr), pp. 457-502. Weinheim, Germany: Wiley-VCH Verlag GmbH & Co.

HUNG, W. C., LEE, M. T., CHEN, F. Y. & HUANG, H. W. (2007). The condensing effect of cholesterol in lipid bilayers. Biophys J, 92(11), 3960-3967.

HUNG, W. C., LEE, M. T., CHUNG, H., SUN, Y. T., CHEN, H., CHARRON, N. E. & HUANG, H. W. (2016). Comparative Study of the Condensing Effects of Ergosterol and Cholesterol. Biophys J, 110(9), 2026-2033.

KUMAR, S., ed. (2001). Liquid Crystals: Cambridge University Press.

KWOK, R. & EVANS, E. (1981). Thermoelasticity of large lecithin bilayer vesicles. Biophys J, 35(3), 637-652.

LEE, C. C., SUN, Y., QIAN, S. & HUANG, H. W. (2011). Transmembrane pores formed by human antimicrobial peptide LL-37. Biophys J, 100(7), 1688-1696.
LEE, M. T., HUNG, W. C., CHEN, F. Y. & HUANG, H. W. (2008). Mechanism and kinetics of pore formation in membranes by water-soluble amphipathic peptides. Proc Natl Acad Sci U S A, 105(13), 5087-5092.
LEE, M. T., SUN, T. L., HUNG, W. C. & HUANG, H. W. (2013). Process of inducing pores in membranes by melittin. Proc Natl Acad Sci U S A, 110(35), 14243-14248.
LEVINE, Y. K. & WILKINS, M. H. (1971). Structures of oriented lipid bilayers. Nature New Biology, 230, 69-72.
LONGO, M. L., WARING, A. J., GORDON, L. M. & HAMMER, D. A. (1998). Area expansion and permeation of phospholipid membrane bilayer by influenza fusion peptides and melittin. Langmuir, 14, 2385-2395.
LONGO, M. L., WARING, A. J. & HAMMER, D. A. (1997). Interaction of the influenza hemagglutinin fusion peptide with lipid bilayers: area expansion and permeation. Biophys J, 73(3), 1430-1439.
LUDTKE, S., HE, K. & HUANG, H. (1995). Membrane thinning caused by magainin 2. Biochemistry, 34(51), 16764-16769.
LUDTKE, S. J., HE, K., WU, Y. & HUANG, H. W. (1994). Cooperative membrane insertion of magainin correlated with its cytolytic activity. Biochim Biophys Acta, 1190(1), 181-184.
MARTIN, O. C. & PAGANO, R. E. (1987). Transbilayer movement of fluorescent analogs of phosphatidylserine and phosphatidylethanolamine at the plasma membrane of cultured cells. Evidence for a protein-mediated and ATP-dependent process(es). J Biol Chem, 262(12), 5890-5898.
MOFFITT, W. (1956). Optical Rotatory Dispersion of Helical Polymers. Journal of Chemical Physics, 25(3), 467-478.
OLAH, G. A. & HUANG, H. W. (1988a). Circular-Dichroism of Oriented Alpha-Helices .2. Electric-Field Oriented Polypeptides. Journal of Chemical Physics, 89(11), 6956-6962.
OLAH, G. A. & HUANG, H. W. (1988b). Circular dichroism of oriented α-helices. J. Chem. Phys., 89, 2531-2538.
OLAH, G. A., HUANG, H. W., LIU, W. H. & WU, Y. L. (1991). Location of ion-binding sites in the gramicidin channel by X-ray diffraction. J Mol Biol, 218(4), 847-858.
POWERS, L. & PERSHAN, P. S. (1977). Monodomain samples of dipalmitoyl phosphatidylcholine with varying concentrations of water and other ingredients. Biophys J, 20(2), 137-152.
QIAN, S., WANG, W., YANG, L. & HUANG, H. W. (2008). Structure of the alamethicin pore reconstructed by X-ray diffraction analysis. Biophys J, 94, 3512-3522.
RODRIGUEZ, N., HEUVINGH, J., PINCET, F. & CRIBIER, S. (2005). Indirect evidence of submicroscopic pores in giant unilamellar [correction of unilamelar] vesicles. Biochim Biophys Acta, 1724(3), 281-287.
ROTHSCHILD, K. J., SANCHES, R., HSIAO, T. L. & CLARK, N. A. (1980). A spectroscopic study of rhodopsin alpha-helix orientation. Biophys J, 31(1), 53-64.
SEIGNEURET, M. & DEVAUX, P. F. (1984). ATP-dependent asymmetric distribution of spin-labeled phospholipids in the erythrocyte membrane: relation to shape changes. Proc Natl Acad Sci U S A, 81(12), 3751-3755.
SUN, Y., HUNG, W. C., CHEN, F. Y., LEE, C. C. & HUANG, H. W. (2009). Interaction of tea catechin (-)-epigallocatechin gallate with lipid bilayers. Biophys J, 96(3), 1026-1035.
SUN, Y., SUN, T. L. & HUANG, H. W. (2016). Mode of Action of Antimicrobial Peptides on E. coli Spheroplasts. Biophys J, 111(1), 132-139.
TAMBA, Y., ARIYAMA, H., LEVADNY, V. & YAMAZAKI, M. (2010). Kinetic pathway of antimicrobial peptide magainin2 induced pore formation in lipid membranes. J. Phys. Chem. B, 114, 12018-12026.

TAMBA, Y. & YAMAZAKI, M. (2005). Single giant unilamellar vesicle method reveals effect of antimicrobial peptide magainin 2 on membrane permeability. Biochemistry, 44(48), 15823-15833.
TAMM, L. K. & TATULIAN, S. A. (1997). Infrared spectroscopy of proteins and peptides in lipid bilayers. Q Rev Biophys, 30(4), 365-429.
TINOCO, I., JR. (1964). Circular dichroism and rotatory dispersion curves of helices. J. Am. Chem. Soc., 86, 297-298.
TORBET, J. & WILKINS, M. H. (1976). X-ray diffraction studies of lecithin bilayers. J Theor Biol, 62(2), 447-458.
VELLUZ, L., LEGRAND, M. & GROSJEAN, M. (1965). Optical circular dichroism. New York: Academic Press.
WANG, W., PAN, D., SONG, Y., LIU, W., YANG, L. & HUANG, H. (2006). Method of x-ray anomalous diffraction for lipid structures. Biophys J, 91, 736-743.
WARREN, B. E. (1990). X-ray Diffraction. Mineola, N.Y.; pp. 41-47, 51-54.: Dover Publications,.
WEISS, T. M., VAN DER WEL, P. C., KILLIAN, J. A., KOEPPE, R. E., 2ND & HUANG, H. W. (2003). Hydrophobic mismatch between helices and lipid bilayers. Biophys J, 84(1), 379-385.
WEISS, T. M., YANG, L., DING, L., WARING, A. J., LEHRER, R. I. & HUANG, H. W. (2002). Two states of cyclic antimicrobial peptide RTD-1 in lipid bilayers. Biochemistry, 41(31), 10070-10076.
WOODY, R. W. (1985). Circular dichroism of peptides. In The Peptides eds. S. Udenfriend and J. Meienhofler), pp. 15-114. New York: Academic Press.
WOODY, R. W. (1993). The circular dichroism of oriented beta sheets: theoretical predictions. Tetrahedron Asymmetry, 4, 529-544.
WU, Y., HUANG, H. W. & OLAH, G. A. (1990). Method of oriented circular dichroism. Biophys J, 57, 797-806.
YAMAOKA, K., UEDA, K. & KOSAKO, I. (1986). Far-Ultraviolet Electric Linear Dichroism .3. Far-Ultraviolet Electric Linear Dichroism of Poly(Gamma-Methyl L-Glutatmate) in Hexafluoro-2-Propanol and the Peptide Band in the 187-250-Nm Wavelength Region. Journal of the American Chemical Society, 108(15), 4619-4625.
YANG, L., HARROUN, T. A., HELLER, W. T., WEISS, T. M. & HUANG, H. W. (1998). Neutron off-plane scattering of aligned membranes. I. Method Of measurement. Biophys J, 75(2), 641-645.
YANG, L., HARROUN, T. A., WEISS, T. M., DING, L. & HUANG, H. W. (2001). Barrel-stave model or toroidal model? a case study on melittin pores. Biophys J, 81, 1475-1485.
YANG, L. & HUANG, H. W. (2003). A rhombohedral phase of lipid containing a membrane fusion intermediate structure. Biophys J, 84(3), 1808-1817.